Shape Recognition Using the Eigenvalues of the Laplacian and other Operators

Lotfi Hermi, University of Arizona

Based on joint theoretical work with **E. M. Harrell** (Georgia Tech) and applications with
M. A. Khabou (U. W. Florida) and **M. B. H. Rhouma** (SQU, Oman)

Outline:

(1) Inferring shape from physical attributes (vibration modes)
(2) Positive and negative answers
(3) Eigenvalue-based feature functions
(4) Application to Shape Recognition
(5) Other eigenvalue problems

(1) Inferring Shape from Vibration Modes of a Drum:

This is the old famous question of M. Kac (1966):
"Can one hear the shape of a drum?"

Consider planar domain Ω
(or a general Ω domain in d-dimensions)

Can one determine the shape of the domain?

Fixed Membrane Problem:

$$-\Delta u = \lambda \ u \quad in \quad \Omega$$
$$u = 0 \quad on \quad \partial\Omega$$

Eigenmodes: $0 < \lambda_1 < \lambda_2 \le \lambda_3 \le \cdots$

Eigenfunctions: $u_1, u_2, u_3, \cdots$.

Weyl (1910)

$$\lambda_k \sim \frac{4\pi^2 k^{2/d}}{(C_d|\Omega|)^{2/d}} = \frac{k^{2/d}}{\left(L_{0,d}^{cl}|\Omega|\right)^{2/d}} \quad as \quad k \to \infty,$$

$$N(z) \sim L_{0,d}^{cl}\, z^{d/2}\, |\Omega| \quad as \quad z \to \infty$$

Here $C_d = \dfrac{\pi^{d/2}}{\Gamma(d/2+1)}$ = volume of the $d-$Ball.
Also, $L_{0,d}^{cl} = C_d/(2\pi)^d$.

For good reviews of the history of these asymptotics (and extensive literature and extensions to various operators), see Birman and Solomyak (period 67-75), Clark (pre-1967): Titchmarch, Hörmander, Levitan, Agmon, Browder, Gârding, V.A. Il'in, Carleman, Pleijel, Naimark, Kac, Ray, etc.

The Counting function=staircase function

$$N(z) = \sum_{\lambda_k \le z} 1 = \sup_{\lambda_k \le z} k.$$

By convention, this is sometimes written as

$$N(z) = \sum_k (z - \lambda_k)_+^0$$

to parallel the definition of the Riesz mean of order $\rho > 0$

$$R_\rho(z) = \sum_k (z - \lambda_k)_+^\rho .$$

In fact the two are related by the *Riesz iteration* (also called *Aizenman-Lieb procedure*)

$$R_\rho(z) = \rho \int_0^\infty (z - t)_+^{\rho - 1} N(t) dt.$$

The Riesz mean is a "smoothed staircase" function.

In fact:

$$R_{\sigma+\delta}(z) = \frac{\Gamma(\sigma+\delta+1)}{\Gamma(\sigma+1)\,\Gamma(\delta)} \int_0^\infty (z-t)_+^{\delta-1} R_\sigma(t)dt.$$

This is the *Riemann-Liouville fractional transform*.

Also interest in

$$Z(t) = \text{ partition function } = \sum_{k=1}^{\infty} e^{-\lambda_k t}.$$

$$\zeta_{spec}(\rho) = \text{ spectral zeta function } = \sum_{k=1}^{\infty} \frac{1}{\lambda_k^\rho}.$$

Why interest in all of these spectral functions: Information about one leads to information about others, giving further insight into the nature of the spectrum

$$N(z) \sim L_{0,d}^{cl} z^{d/2} |\Omega| \text{ as } z \to \infty$$

Applying (heuristically) the Laplace transform

$$\mathcal{L}\{f\}(t) = \int_0^\infty f(z) e^{-zt} dz.$$

one obtains

$$Z(t) = \sum_{k=1}^{\infty} e^{-\lambda_k t} \sim \frac{|\Omega|}{(4\pi t)^{d/2}}.$$

Forward transforms are "easy": integral transforms

Inverse transforms ("hard analysis"): Tauberian theorems

$$N(z) \sim L^{cl}_{0,d}\, z^{d/2}\, |\Omega| \text{ as } z \to \infty$$

If one applies Riesz iteration, one is led to

$$R_\rho(z) \sim L^{cl}_{\rho,d}\, z^{\rho+d/2}\, |\Omega| \text{ as } z \to \infty$$

where $L^{cl}_{\rho,d} = \dfrac{\Gamma(1+\rho)}{(4\pi)^{d/2}\,\Gamma(1+\rho+d/2)}$.

$z \to \infty$ corresponds to $t \to 0+$

There are well-known isoperimetric results (for λ_1, λ_2/λ_1, etc.)

Rayleigh-Faber-Krahn,
Ashbaugh-Benguria-PPW,
Payne-Weinberger, etc.

Queen Dido (Carthaginian coin, circa 200 BC, modern Tunisia)

Universal Inequalities

- PPW (1956)

$$\lambda_{k+1} - \lambda_k \leq \frac{4}{d}\overline{\lambda_k}$$

- Hile-Protter refinement (1980)

- H. C. Yang (1991)

$$\sum_{i=1}^{k} (\lambda_{k+1} - \lambda_i)^2 \leq \frac{4}{d} \sum_{i=1}^{k} \lambda_i (\lambda_{k+1} - \lambda_i)$$

- Harrell-Stubbe (1997): For $\rho \geq 2$ (see Ashbaugh-H., 1999)

$$\sum_{i=1}^{k} (\lambda_{k+1} - \lambda_i)^\rho \leq \frac{2\rho}{d} \sum_{i=1}^{k} \lambda_i (\lambda_{k+1} - \lambda_i)^{\rho-1}$$

- For $0 \leq \rho \leq 2$

$$\sum_{i=1}^{k} (\lambda_{k+1} - \lambda_i)^\rho \leq \frac{4}{d} \sum_{i=1}^{k} \lambda_i (\lambda_{k+1} - \lambda_i)^{\rho-1}$$

Universal Inequalities of Weyl-Type

- PPW, 1956

$$\frac{\lambda_{k+1}}{\lambda_k} \leq \left(1 + \frac{4}{d}\right)$$

- Ashbaugh-Benguria (91, 92, 93)

$$\frac{\lambda_{2^m}}{\lambda_1} \leq \left(\frac{j^2_{d/2,1}}{j^2_{d/2-1,1}}\right)^m .$$

While optimal for low-lying eigenvalues, this is not of Weyl-type since the right side of the inequality behaves like $k^{5.77078/d}$ as $k \to \infty$.

- (H. '04, TAMS '08)

$$\frac{\lambda_{k+1}}{\lambda_1} \leq 1 + \left(1 + \frac{d}{2}\right)^{2/d} H_d^{2/n}\, k^{2/d},$$

$$\frac{\overline{\lambda}_k}{\lambda_1} \leq 1 + \frac{H_d^{2/d}}{1 + \frac{2}{d}} k^{2/d}$$

- Cheng and Yang (2007)

$$\frac{\lambda_{k+1}}{\lambda_1} \leq \left(1 + \frac{4}{d}\right) k^{\frac{2}{d}}$$

- Harrell-H. (JFA '08): For $k \geq j \frac{1+\frac{d}{2}}{1+\frac{d}{4}}$,

$$\overline{\lambda_k}/\overline{\lambda_j} \leq 2\left(\frac{1 + \frac{d}{4}}{1 + \frac{d}{2}}\right)^{1+\frac{2}{d}} \left(\frac{k}{j}\right)^{\frac{2}{d}}.$$

- Harrell-H. (JFA '08): For $k \geq j \geq 1$,

$$\lambda_{k+1}/\overline{\lambda_j} \leq \left(1 + \frac{4}{d}\right)\left(\frac{k}{j}\right)^{\frac{2}{d}}.$$

(2) Positive and Negative Results (for hearing the shape of a drum)

- Milnor pair of 16-dimensional tori that have the same eigenvalues but different shapes.
- Bilby and Hawk: Gordon, Webb, and Wolpert (1992). These are a pair of regions in the plane that have different shapes but identical eigenvalues (for the membrane problem)
- Buser, Conway, Doyle (1994) constructed numerous examples of isospectral domains.

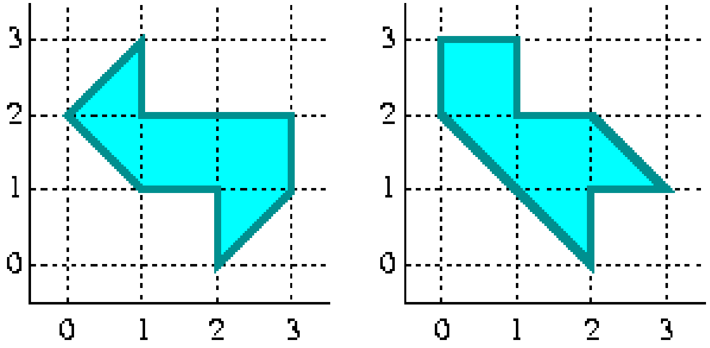

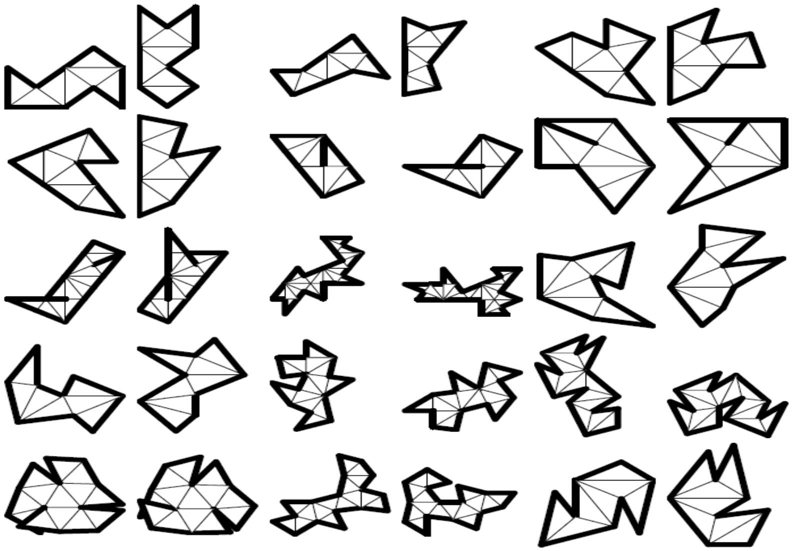

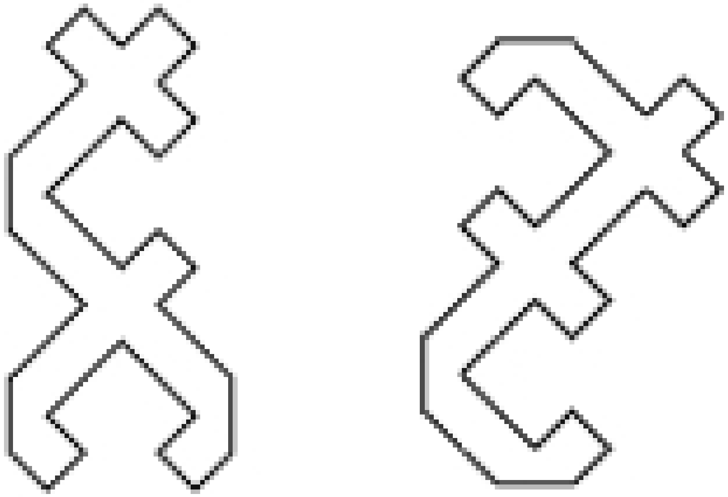

P. Bérard
Transplantation et isospectralité I, II
(1992, 1993)

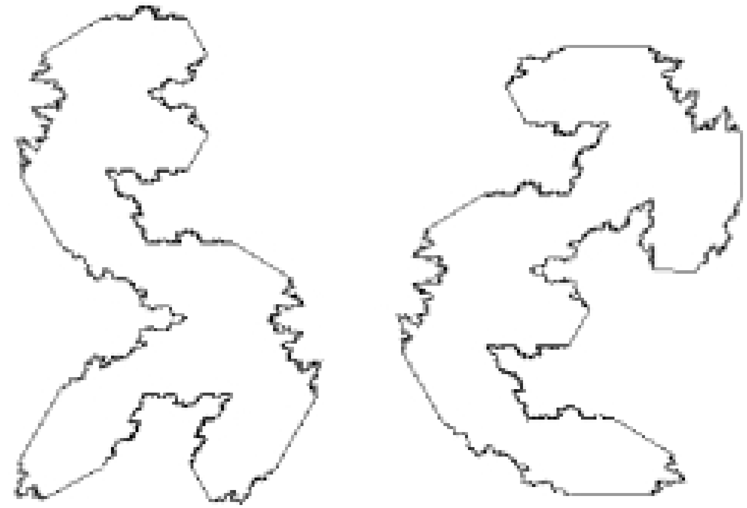

Sleeman-Hua
nonisometric isospectral connected fractal domains (1998, 2000)

H. Urakawa
Bounded domains which are isospectral but not congruent (early 80s)

Driscoll-Gottlieb
Isospectral shapes with Neumann and alternating boundary conditions (2003)

S. Zelditch (GAFA '00, announcement in Math. Research Letters, '99): Under generic conditions, for family of bounded, simply connected real analytic plane domains with four-fold symmetry (symmetry of an ellipse), the spectrum uniquely determines the underlying domain (up to rigid motion).

(3) Eigenvalue–based feature functions

Key properties:

- Invariance under rigid motion (translation, rotation)
  - Domain monotonicity: If $\Omega_1 \subset \Omega_2$ then $\lambda_k(\Omega_1) \geq \lambda_k(\Omega_2)$
    - For $\alpha > 0$, $\lambda_k(\alpha\Omega) = \dfrac{\lambda_k(\Omega)}{\alpha^2}$
      - Scale invariance: $\dfrac{\lambda_k(\alpha\Omega)}{\lambda_m(\alpha\Omega)} = \dfrac{\lambda_k(\Omega)}{\lambda_m(\Omega)}$

Shape Recognition

- Shape Recognition is a key component of object recognition, matching and analysis.
- Invariance under scaling and rigid motion & tolerance to noise and reasonable deformations are the key requirements in a good shape recognition method
- Use shape functions based on ratios of e-values
- Use a finite difference scheme to compute the e-values

For a given binary image assuming the shape of Ω, consider extracting 4 sets of features:

$$F_1(\Omega) \equiv \left\{ \left(\frac{\lambda_1}{\lambda_2}, \frac{\lambda_1}{\lambda_3}, \frac{\lambda_1}{\lambda_4}, \dots, \frac{\lambda_1}{\lambda_n} \right) \right\}$$

$$F_2(\Omega) \equiv \left\{ \left(\frac{\lambda_1}{\lambda_2}, \frac{\lambda_2}{\lambda_3}, \frac{\lambda_3}{\lambda_4}, \dots, \frac{\lambda_{n-1}}{\lambda_n} \right) \right\}$$

$$F_3(\Omega) \equiv \left\{ \left(\frac{\lambda_1}{\lambda_2} - \frac{d_1}{d_2}, \frac{\lambda_1}{\lambda_3} - \frac{d_1}{d_3}, \frac{\lambda_1}{\lambda_4} - \frac{d_1}{d_4}, \dots, \frac{\lambda_1}{\lambda_n} - \frac{d_1}{d_n} \right) \right\}$$

where $n =$ the number of features

$d_1 < d_2 \le d_3 \le \dots \le d_n$ are the first n e-values of a disk.

$$F_4(\Omega) \equiv \left\{ \left(\frac{\lambda_2}{\lambda_1}, \frac{\lambda_3}{2\lambda_1}, \dots, \frac{\lambda_{k+1}}{k\,\lambda_1}, \dots, \frac{\lambda_{n+1}}{n\,\lambda_1} \right) \right\}$$

F4 suggested by the recent work with E. M. Harrell

General schemes takes the form

$$\mathcal{L}_{ij}\ u = \lambda\ \mathcal{R}_{ij}\ u.$$

In the first scheme, $\mathcal{L}_{ij}\ u$ and $\mathcal{R}_{ij}\ u$ are given by

$$\mathcal{L}_{ij}\ u \ = \ \frac{1}{h^2}\left(u_{i+1,j} + u_{i,j+1} + u_{i-1,j} + u_{i,j-1} - 4\ u_{ij}\right),$$

$$\mathscr{R}_{ij}u = -\frac{1}{12}(6u_{ij} + u_{i+1,j} + u_{i,j+1} + u_{i-1,j} + u_{i-1,j-1} + u_{i,j-1}).$$

In the second scheme, $\mathcal{L}_{ij}\ u$ and $\mathcal{R}_{ij}\ u$ take the forms,

$$\mathcal{L}_{ij}\ u = \frac{1}{3h^2}\left(u_{i+1,j} + u_{i,j+1} + u_{i-1,j} + u_{i,j-1} - 8u_{ij}\right),$$

$$\mathscr{R}_{ij}u = -\frac{1}{36}(16u_{ij} + 4_{ui+1,j} + 4u_{i,j+1} + 4u_{i-1,j} + 4u_{i,j-1} + u_{i+1,j+1} + u_{i+1,j-1} + u_{i-1,j+1} + u_{i-1,j-1}).$$

Method & Results

- We use elementary neural networks.
- We train with 50% of the database.
- Simple hand-drawn shapes, synthetic shapes, and real leaves

Hand-drawn shapes

Classification results of the hand-drawn shapes

	F_1 features	F_2 features	F_3 features
Number of features used	12	12	8
Correct classification rate (%)	94.5	93.5	94.0

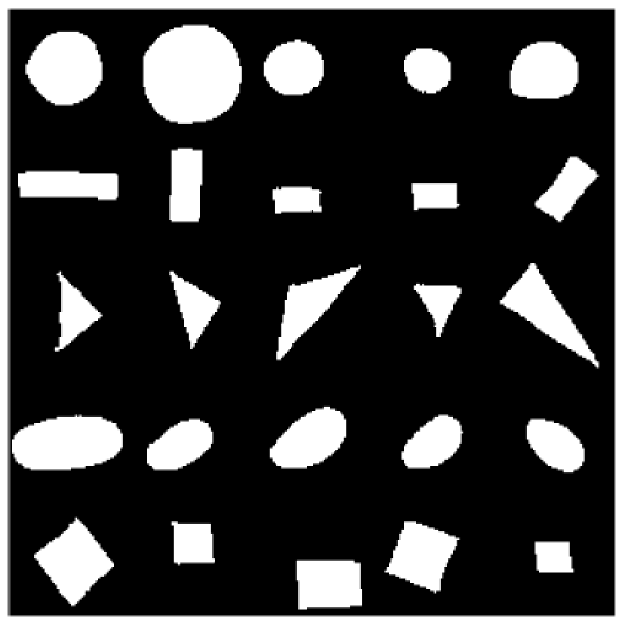

Synthetic Images: Petals

Classification results of the n-petal images ($n = 3, \ldots, 7$)

Number of features	F_1 features (%)	F_2 features (%)	F_3 features (%)
4	70.5	65	74.5
8	79.5	83	88.5
12	93	90	92
16	95	89	92
20	97.5	88	94.5

$$r = a + \varepsilon \cos\theta + \cos n\theta.$$

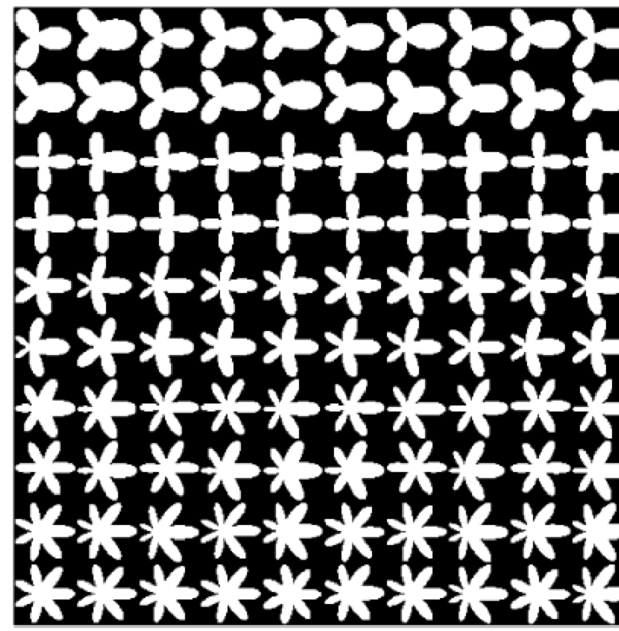

Leaves database

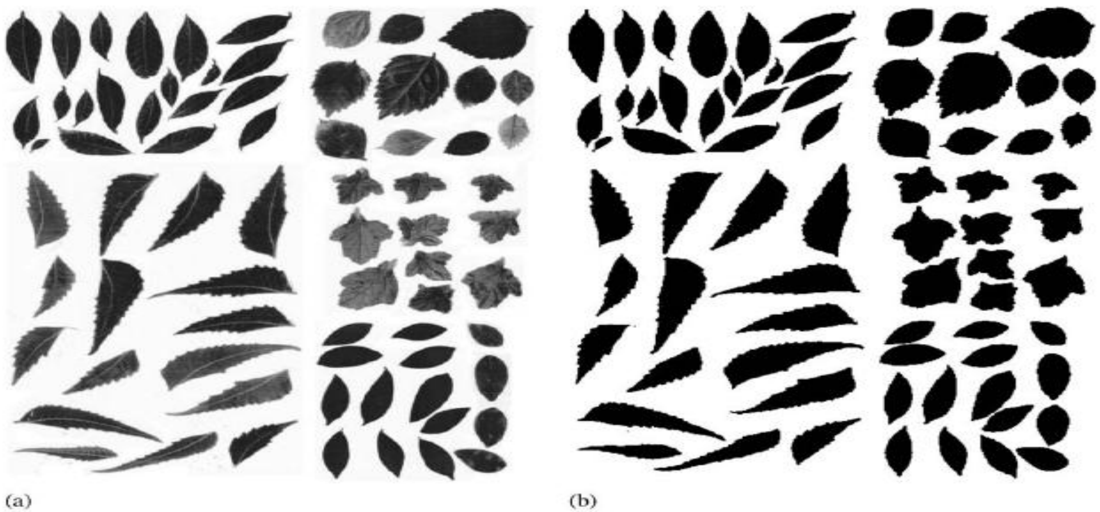

Fig. 13. Picture of the leaves from five different types of trees: (a) gray-scale; (b) thresholded.

Classification results of leaf images

	F_1 features	F_2 features	F_3 features
Number of features used	2	4	2
Correct classification rate (%)	88.9	84.7	88.9

Other Eigenvalue Problems

- Free (or Neumann) Membrane Problem:

$$-\Delta u = \mu \; u \quad in \quad \Omega$$
$$\frac{\partial u}{\partial n} = 0 \quad on \quad \partial\Omega$$

Eigenmodes: $0 = \mu_0 < \mu_1 \leq \mu_2 \leq \cdots$

- Steklov Problem:

$$\Delta u = 0 \quad in \quad \Omega$$
$$\frac{\partial u}{\partial n} = \lambda \; u \quad on \quad \partial\Omega$$

Eigenmodes: $0 = \lambda_0 < \lambda_1 \leq \lambda_2 \leq \cdots$

- Clamped Plate Problem:

$$\Delta^2 u = \Gamma \, u \text{ in } \Omega, \qquad u = \frac{\partial u}{\partial n} = 0 \text{ on } \partial\Omega$$

- The eigenvalues

$$0 < \Gamma_1 \leq \Gamma_2 \leq \ldots \leq \Gamma_k \to \infty$$

satisfy two key properties. For $\alpha > 0$ and for $\alpha\Omega$ denoting he scaling of the domain Ω by α:

- $\Gamma_k(\alpha\Omega) = \dfrac{\Gamma_k(\Omega)}{\alpha^4}$
- $\dfrac{\Gamma_k(\alpha\Omega)}{\Gamma_m(\alpha\Omega)} = \dfrac{\Gamma_k(\Omega)}{\Gamma_m(\Omega)}$

- Buckling Plate Problem:

$$\Delta^2 u = \Lambda \, \Delta u \text{ in } \Omega, \qquad u = \frac{\partial u}{\partial n} = 0 \text{ on } \partial\Omega$$

- $\Lambda_k(\alpha\Omega) = \dfrac{\Lambda_k(\Omega)}{\alpha^2}$
- $\dfrac{\Lambda_k(\alpha\Omega)}{\Lambda_m(\alpha\Omega)} = \dfrac{\Lambda_k(\Omega)}{\Lambda_m(\Omega)}$

There are well-established finite difference schemes.

There are well-known semiclassical asymptotics as well as universal eigenvalues for the eigenvalues and for various spectral functions

One can use the same feature functions.

	Dirichlet		Neumann		Stekloff	
n	F_1	F_2	F_1	F_2	F_1	F_2
4	60.0%	91.0%	87.5%	91.0%	40.5%	34.0%
8	94.0%	94.0%	94.0%	94.0%	45.0%	41.5%
12	94.5%	93.5%	94.5%	94.0%	50.0%	42.0%
16	92.5%	78.5%	92.5%	91.0%	61.0%	57.5%
20	95.5%	94.5%	95.5%	94.5%	55.5%	56.0%

Correct classification rates of hand-drawn shapes using Dirichlet, Neumann, and Stekloff F1 and F2 features.

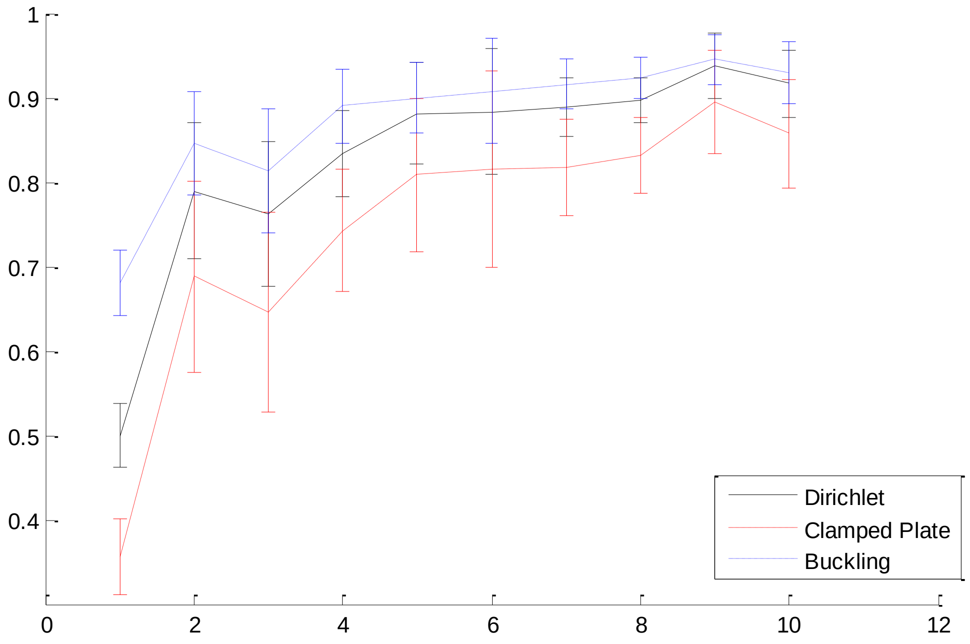

Average and std dev of first 10 F2 features of 100 triangles using Dirichlet, Clamped plate and Buckling eigenvalues

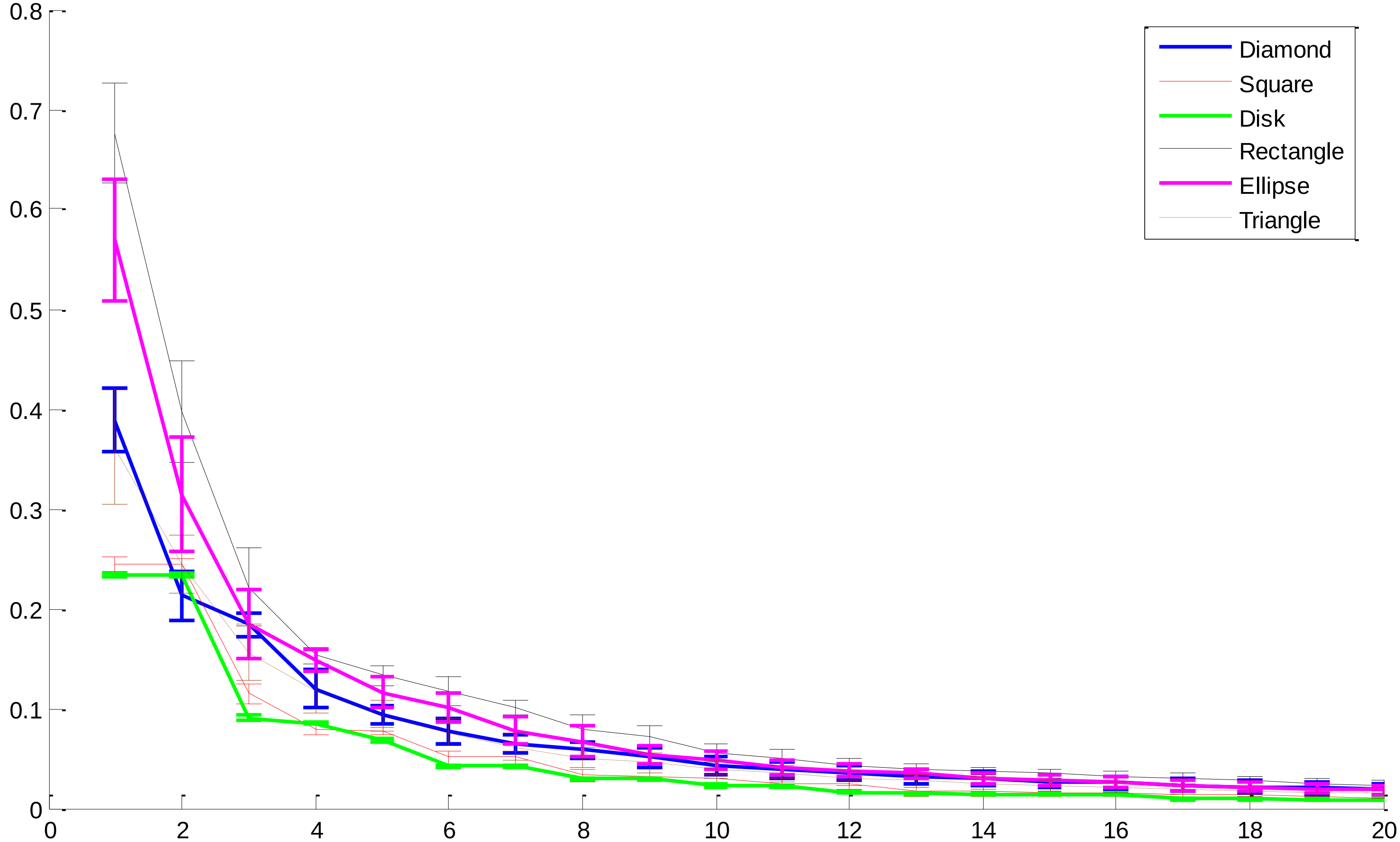

Average and std dev of first 20 F1 features for basic shapes using clamped plate eigenvalues

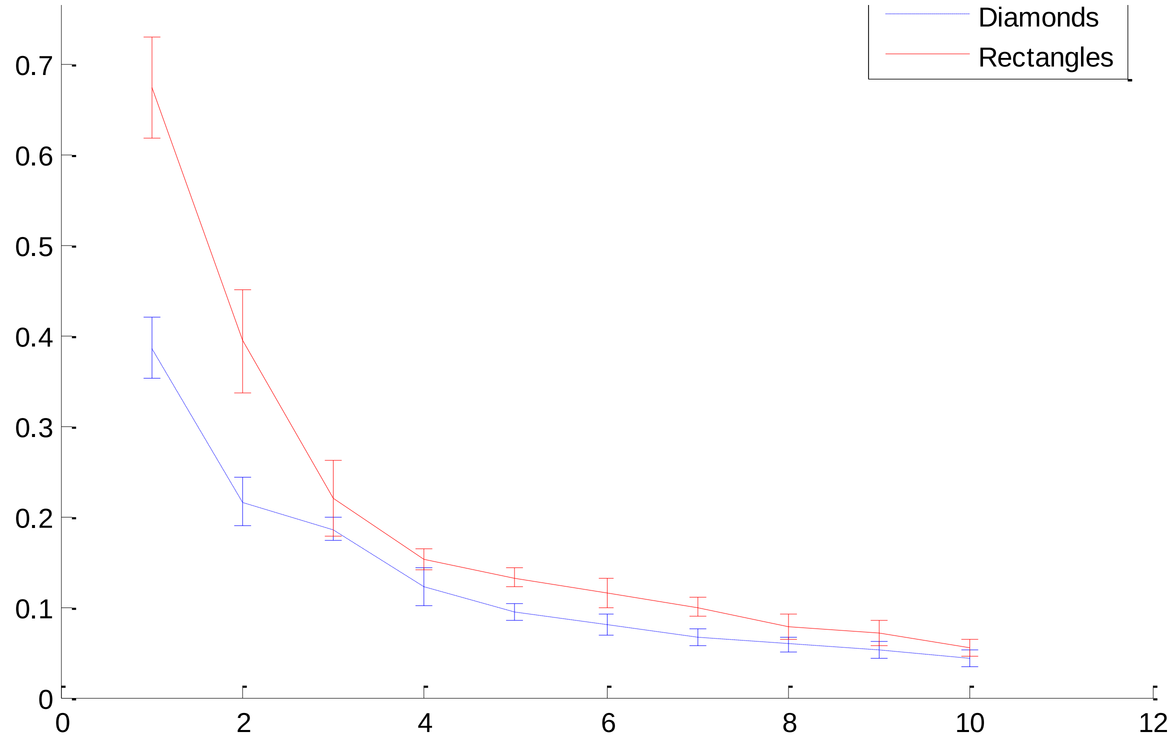

Average and std dev of first 10 F1 features of 100 rectangles and diamonds computed using Dirichlet and clamped plate eigenvalues

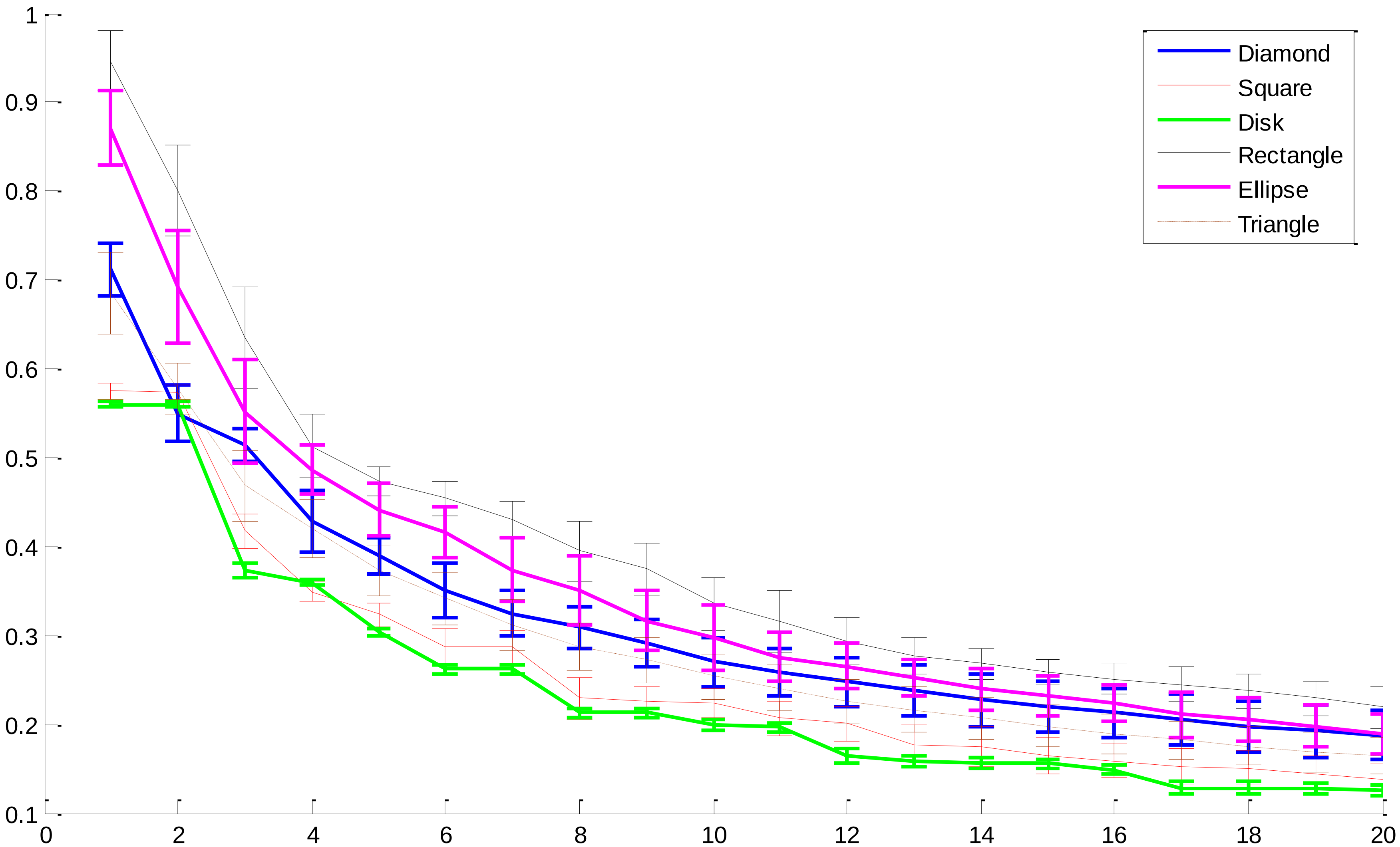

Average and std dev of first 20 F1 features for basic shapes using buckling plate eigenvalues

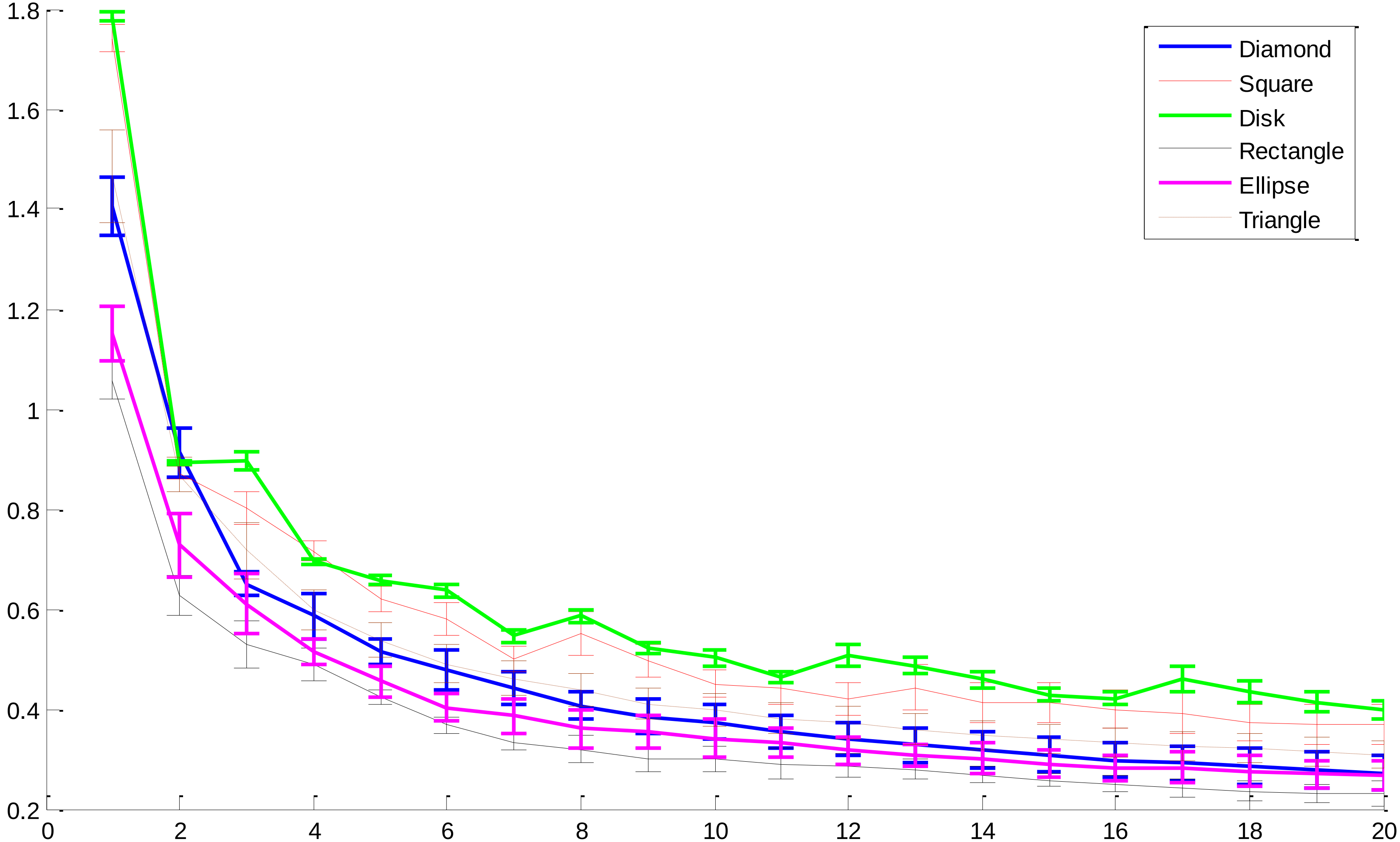

Average and std dev of first 20 F4 features using buckling plate eigenvalues

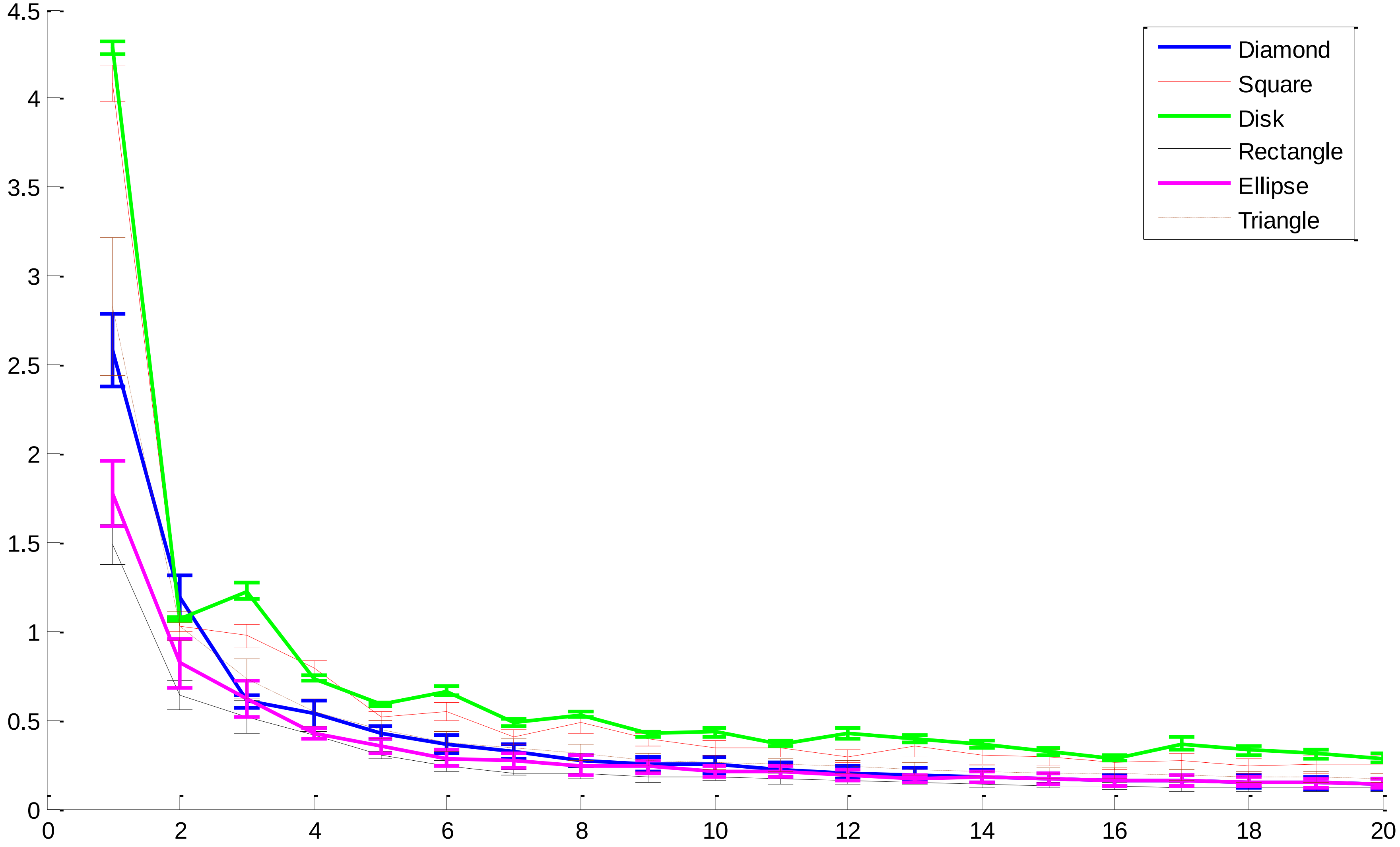

Average and std dev of first 20 F4 features using clamped plate eigenvalues

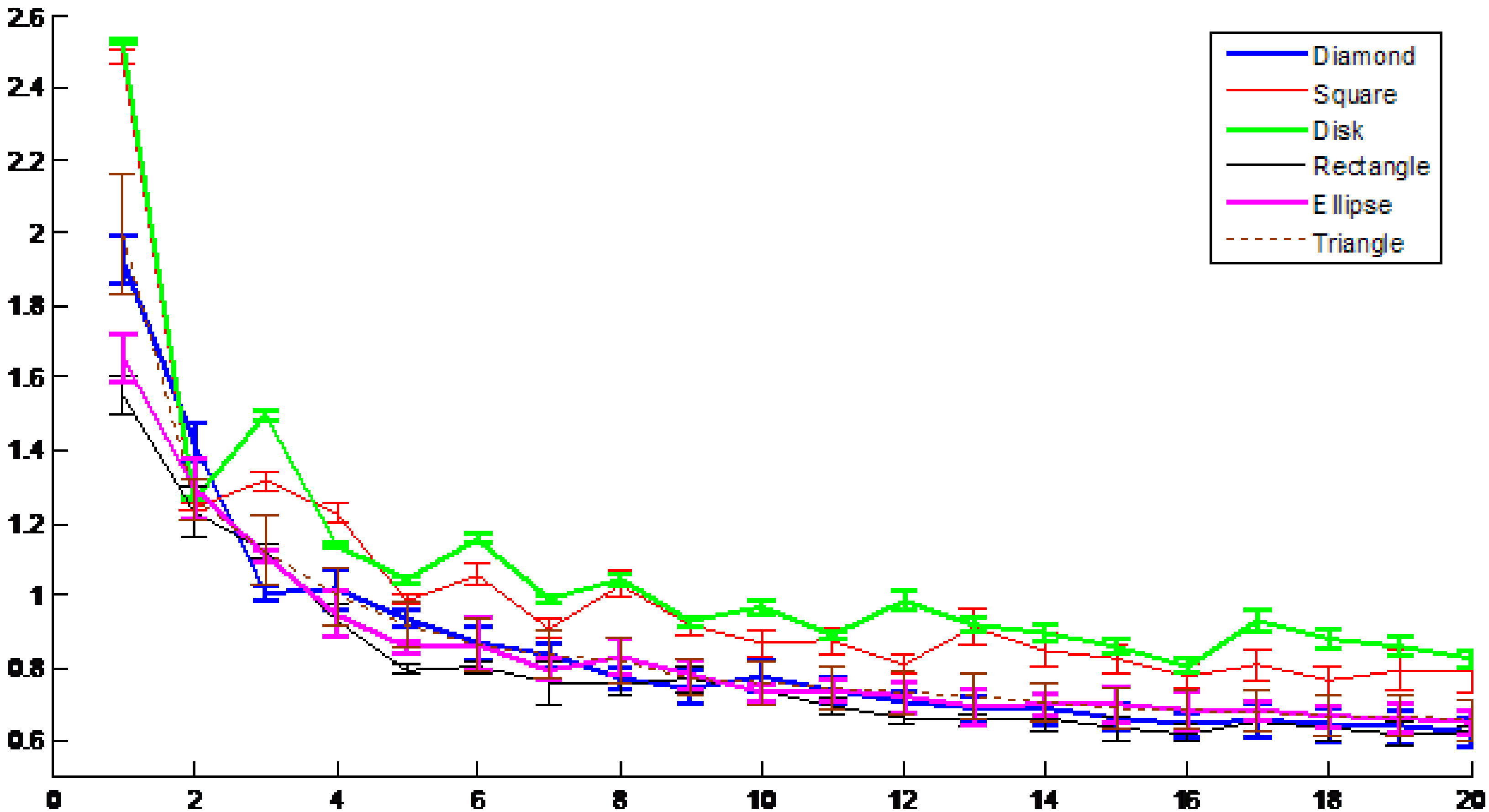

Average and std dev of first 20 F4 features using Dirichlet eigenvalues